Preparation and Properties of *in situ* Polymerized Poly(ethylene terephthalate)/Fumed Silica Nanocomposites

Wan-Gyu Hahm, Hee-Soo Myung, and Seung Soon Im*

Department of Textile and Polymer Engineering, College of Engineering, Hanyang University, Haengdang-dong, Seungdong-ku, Seoul 133-791, Korea

Abstract: We have prepared poly(ethylene terephthalate) (PET) nanocomposites filled with two different types of fumed silicas, hydrophilic (FS) and hydrophobic (MFS) silicas of 7-nm diameter, by *in situ* polymerization. We then investigated the morphological changes, rheological properties, crystallization behavior, and mechanical properties of the PET nanocomposites. Transmission electron microscopy (TEM) images indicate that the dispersibility of the fumed silica was improved effectively by *in situ* polymerization; in particular, MFS had better dispersibility than FS on the non-polar PET polymer. The crystallization behavior of the nanocomposites revealed a peculiar tendency: all the fillers acted as retarding agents for the crystallization of the PET nanocomposites. The incorporation of fumed silicas increased the intrinsic viscosities (IV) of the PET matrix, and the strong particleparticle interactions of the filler led to an increased melt viscosity. Additionally, the mechanical properties, toughness, and modulus of the nanocomposites all increased, even at low filler content.

Keywords: poly(ethylene terephthalate), nanocomposite, fumed silica, *in situ* polymerization.

Introduction

Recently, with the successful development of the nanotechnologies, various inorganic nano-particles such as layered silicates and carbon nano-tube have attracted much attention, and many research groups have reported that polymer composites filled with those nano-particles have unique properties: increase of mechanical properties,[1,2] improvement of chemical and thermal resistance,[3-5] and enhancement of gas barrier[6] at the low filler content. The achievement of these properties strongly depends on many factors including the wettability and chemical bond at the interface between filler and matrix, and the filler dispersibility on the matrix. These difficult factors have still restricted the employment of inorganic nano-particles to polymer.

Fumed silicas have an extremely large surface area per the unit weight and numerous silanol groups (Si-OH) on the surface.[7] Owing to these characteristics, the fumed silica shows hydrophilicity and exhibits a very high surface energy leading to the aggregates and particle-particle interaction of filler in non-polar liquids.[8] Thus, the silanol groups on its surface can be chemically modified into various methylsilyl groups to reduce the surface energy and the hydrophobic

property could be obtained.[9,10] Barthel[8] found that the particle-particle interaction of inorganic filler is heavily related with the polarity of liquid medium, and Chung *et al.*[11] confirmed that the incorporation of the surface modified silica affect the dispersibility of silica in non-polar polymer matrix.

Accordingly, considering effective dispersibility of silica, one proposed that *in situ* polymerization can be applied as an effective method to prepare the polymer nanocomposite filled with fumed silicas. Some research groups have studied the characteristics of thermoplastic polymer-fumed silica nanocomposites based on polyamide 6[12,13] and polypropylene[14] via *in situ* polymerization, but there are little systematic researches for PET nanocomposite filled with fumed silica, although poly(ethylene terephthalate) (PET) is one of the most widely used commercial thermoplastic polymers.

In this work, two kind of fumed silicas, hydrophilic/hydrophobic inorganic nano-particles of 7 nm, were used as a filler, and PET-fumed silica nanocomposites were prepared by *in situ* polymerization. The various effects of fumed silicas in the PET matrix as functions of filler type and filler content were studied and compared with the results of former study by direct melt compounding.[11] The degree of particle-particle interaction and dispersion of each fumed silica on PET nonpolar matrix were investigated, and the crystallization behaviors and dynamic rheological properties of nanocomposites due to the improvement of dispersibility for nano-particles

were discussed in detail. Mechanical analyses were also performed to explain the relationship between the structure and properties of these nanocomposites.

Experimental

Materials. Hydrophilic fumed silica (FS) of 7 nm primary particle size was purchased from Sigma, and hydrophobic modified fumed silica (MFS):[10] silanol groups (Si-OH) on the surface of FS were chemically modified into trimethylsilyl groups $(Si-(CH_3)_3)$ of same size was purchased from Degussa. Dimethylterephthalate (DMT) and ethylene glycol (EG) were obtained as ACS grade and used to prepare PET matrix polymer without further purification. More detailed properties of the materials used in this work are given in Table I.

Characterization of Fumed Silicas. The methanol wettability,[15] the degree of hydrophobic/hydrophilic property, of each silica in Table I were measured and calculated with the total volume (mL) of added methanol until the silica of 0.2 g were completely precipitated from the surface of distilled water of 50 mL by stirring.

The existence and degree of particle-particle interactions and packing fractions of each silica in the non-polar matrix were verified by BROOKFIELD viscometer (DV-II) with the spindle type of LV-6. Liquid paraffin (65 cP at 30°C) was used for liquid media, and fumed silicas of each desired weight were added to liquid paraffin of 400 mL. All mixtures were stirred for 30 min at 1,500 rpm by agitator prior to measurement, and the viscosity of the prepared homogeneous mixtures were measured at 30°C within the permissible limits of manual.

Preparation of PET Nanocomposites and Their Characterization. PET/fumed silica nanocomposites were prepared via *in situ* polymerization as functions of filler type (FS and MFS) and filler content (0.5 and 2.0 wt%). The polymerization reaction was carried out in two steps: trans-

esterification and polycondensation. Transesterification was first executed by DMT method at 210°C for 3 h under a nitrogen atmosphere. The mole ratio of DMT:EG was 1:2, and EG slurry containing fumed silica was stirred enough over 1 h at 180 rpm to disperse the silicas prior to the reaction. Polycondensation was then carried out at 287°C and 0.7 Torr for maximum 3 h 30 min in consideration of the increase rate of polymer melt viscosity by torque meter. Zinc acetate $(Zn(CH_3COO)_2 2H_2O)$ and antimony (III) oxide (Sb_2O_3) were used for catalysts of transesterification and polycondensation, and phosphoric acid (H_3PO_4) was used for thermal stabilizer. All fumed silicas were dried for 24 h in a vacuum dryer at 90°C prior to addition.

Intrinsic viscosities (IV) of PET nanocomposites dissolved in tetrachloroethane /phenol (4/6 w/w) were measured with Ubbelohde viscometer at 30°C and 0.5 g/dL concentration. NMR samples were prepared by dissolving PET nanocomposites in trifluoro acetic acid and a small amount of $CDCl_3$, and NMR spectra were measured by fourier transform-NMR (Varian, 300 MHz). Mechanical test were conducted with the tensile testing machine (Instron 4465, Instron Corp.) according to ASTM D882 at a crosshead speed of 50 mm/min.

The dispersibility and aggregation size of fume silicas in PET matrix were examined by transmission electron microscope (TEM, JEOL 2010, 200 kV). Samples for TEM analysis of ultra-thin sections ranging from 40 to 60 nm in thickness were prepared with a diamond knife at a temperature of -40°C using a Reichert-Jung Ultracut E microtome. The morphology of PET nanocomposites film surface, which was treated in NaOH solution of 10 o.w.f (on the weight of fiber/film) % at 80°C for 12 h, was obtained with a field emission scanning electron microscope (FE-SEM, JEOL, JSM-6330F).

The rheological properties at the melt state of the nanocomposites were measured by dynamic oscillatory rheometer (ARES, Rheometric Scientific Inc.) using a 25 mm diameter

Table I. The Materials Used in This Study

Materials	Supplier	Typical Properties (Source: supplier)
Hydrophilic Fumed Silica (FS)	Sigma	Blue-gray powder; Primary particle size: 7 nm; Surface area: 390 ± 40 m²/g; Purity grade: > 99.8%; Hydroxyl groups: 3.5~4.5/nm²; Methanol Wettability[a]: 0%
Hydrophobic Fumed Silica (MFS)	Degussa	Fluffy white powder; Primary particle size: 7 nm; Surface area: 260 ± 30 m²/g; Purity grade: > 99.8%; Methanol Wettability[a]: 41.6%
Dimethylterephthalate (DMT)	Sigma-Aldrich	White briquettes; MW: 194.2; mp: 140~142°C: 99+%
Ethylene Glycol (EG)	Sigma-Aldrich	Colorless liquid; MW: 62.07; Density: 1.113g/mL, 25°C Assay: 99+%; Bp: 196~198°C/760 mm Hg

[a]Methanol wettability(%) = $(A \times 0.79)/(A \times 0.79+50) \times 100$.
-A: Total volume (mL) of added methanol until the filler of 0.2 g was completely precipitated in distilled water of 50 mL.

parallel plate of 1.0 mm gap at 270 °C. The frequency ranged from 0.1 to 400 rad/s. Rheological specimens were dried for 24 h in vacuum oven at 90 °C prior to measurements.

Crystallization behaviors of the samples were measured by Perkin-Elmer DSC 7 under a dry nitrogen atmosphere. All samples for non-isothermal crystallization were first melted at 270 °C for 5 min and then quenched to 30 °C at a rate 500 °C/min to obtain a completely amorphous specimen. The second dynamic scanning of heating and cooling was performed in the range of 30~270 °C at a rate of 10 °C/min. Scanning of isothermal melt-crystallization was carried out at the temperature of 205, 210 and 215 °C. All samples were also melted at 270 °C for 5 min to remove the previous thermal history and quickly cooled at 200 °C/min to the each desired isothermal crystallization temperature. The thermal transitions of isothermal crystallization were recorded as a function of time.

Results and Discussion

Characteristic Properties of Nano Fumed Silicas. In this work, the characteristic properties of each fumed silica were investigated by the methanol wettability and BROOK-FIELD viscometer prior to *in situ* polymerization. As expected, the data of methanol wettability, the degree of hydrophobic/hydrophilic property, for fumed silicas in Table I actually confirm that FS has completely hydrophilic properties but surface modified MFS has hydrophobic property to some degree.

The particle-particle interactions of fumed silicas in the non-polar media were verified by BROOKFIELD viscometer, and Figure 1 shows the variations of viscosity for the liquid paraffin mixtures as functions of filler types, filler contents and RPM of spindle. At the spindle speed of 6 rpm, as the filler content increase, the increasing rate of dynamic viscosity for the mixture containing hydrophilic FS filler (Figure 1(a)) is higher than that for the mixture containing hydrophobic MFS filler (Figure 1(b)). For identical filler content, the viscosity decreased with increasing the spindle speed, and these tendencies are remarkably distinct with increasing filler contents. These would indicate that the particle interactions increase with filler content and can be collapsed by shear force, spindle rpm, in the matrix even at the low filler content,[8] and FS has stronger filler interaction than MFS in the non-polar media because FS has more hydrophilic silanol groups causing the increase of surface energy than MFS in the surface.[9,10] These results also show that the maximum nano filler content influencing the viscosity of composite can be predicted by BROOKFIELD viscometer method.

The Effects of Nano fumed Silica on *In Situ* Polymerization for PET Nanocomposites. First, Figure 2 shows the variations of torque on the shaft of agitator as a function of the reaction time at the polycondensation of PET and its nanocomposites. The increasing rates of torque for all nano-
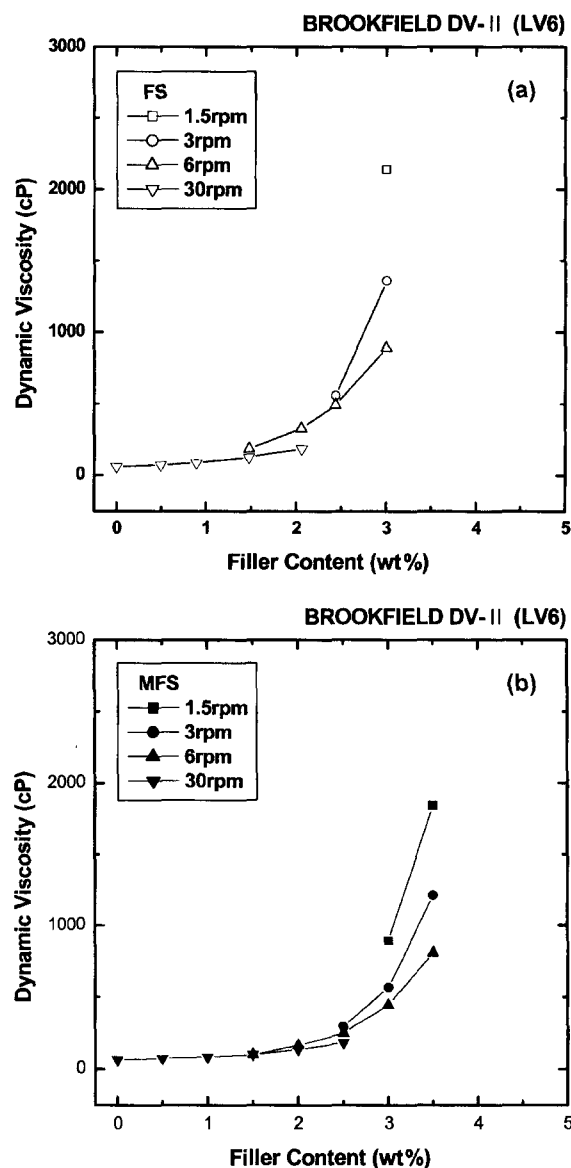

Figure 1. The variations of dynamic viscosity for liquid paraffin/ fumed silica mixtures as a function of filler type and filler content: (a) Paraffin/FS and (b) Paraffin/MFS (Temperature: 30 °C).

composites with reaction time are higher than that of neat PET, and these rates increase more rapidly with the filler contents regardless of filler type. Especially, the increasing rates of torque for nanocomposites filled with FS of 0.5 wt% is higher than those for nanocomposites filled with MFS of 2.0 wt%, and in the case of nanocomposite filled with FS of 2.0 wt%, the torque was too high to agitate at the end of reaction time. Therefore, considering the above results, it appears that the increase of torque for nanocomposites during the polycondensation is caused by fumed silicas on the PET matrix, and these tendencies correspond with those of BROOKFIELD viscometer test.

The IV data of PET and its nanocomposites prepared by *in situ* polymerization in Table II show the effects of fumed silicas for the degree of polymerization of PET. All IV values of nanocomposite are lower than that of neat PET except for the nanocomposite filled with the FS of 0.5 wt% (PET/FS (0.5 wt%)), and these reasons may be that the polycondensation time of all nanocomposites are approximately 1 h shorter than that of neat PET as shown in Figure 2. But, it is interesting that the IV value (0.5255) of PET/FS(0.5 wt%) is higher than that (0.4918) of neat PET and the IV value (0.4675) of PET/MFS(0.5 wt%) is similar than that of neat PET, even if the reaction times of these nanocomposites are shorter than that of neat PET. Besides, all of the IV values of nanocomposites decrease with increasing filler content regardless of filler type at the same reaction time. From these results, it seems that fumed silicas, especially FS, increase the reactivity of molecules on the PET polycondensation
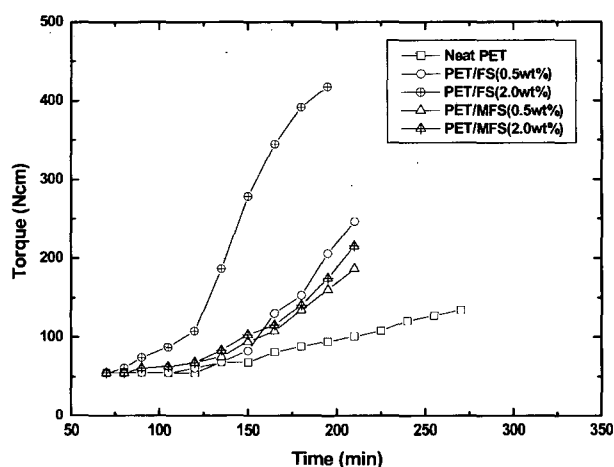
like a catalyst and there is a critical filler content increasing the degree of polymerization of PET, but more additional studies are needed in the future. However, the measurement deviation of original IV values for nanocomposites due to the nano-sized fumed silica in the solutions appears to be little, because there are scarcely any differences between the IV values (0.5053 and 0.4975) of the reference PET solutions, the mixtures of neat PET solution and fumed silicas of 2.0 wt% for the net weight of neat PET, and the IV value (0.4918) of neat PET solution.

The chemical structures of nanocomposites were analyzed by ^{13}C-NMR (Figure 3) to verify the existence of additional chemical bond between the fumed silicas and PET molecules in the nanocomposites, which can influence the increase of the torques and the IV values. But, neat PET and its nanocomposites show the same peaks and there are no peculiar
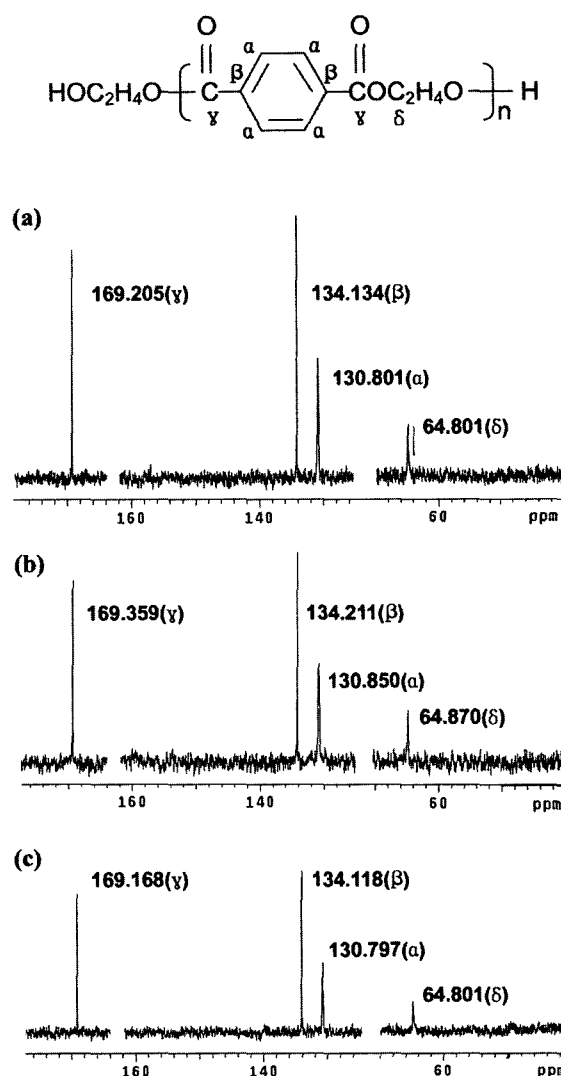

Figure 2. The variations of torque for PET and its nanocomposites as a function of the reaction time at the polycondensation.

Table II. Intrinsic Viscosities (IV) Data of Neat PET and Its Nanocomposites Prepared via *in situ* Polymerization

Sample	IV[a]
Neat PET[b]	0.4918
PET/FS(0.5 wt%)	0.5255
PET/FS(2.0 wt%)	0.3876
PET/MFS(0.5 wt%)	0.4675
PET/MFS(2.0 wt%)	0.4014
PET/FS(2.0 wt%)[c]	0.5053
PET/MFS(0.5 wt%)[d]	0.4975

[a]Intrinsic Viscosity = $(2^{(1/2)}/C) \times (\eta_{sp} - \ln \eta_{rel})^{(1/2)}$; where $\eta_{rel} = t/t_0$, $\eta_{sp} = \eta_{rel} - 1$, and C is polymer concentration (g/dL) in solvent (phenol: tetrachloroethane = 6:4, w/w).
[c,d]The reference PET solutions: the mixtures of neat PET solution[b] and fumed silicas of 2.0 wt% for the weight of neat PET.

Figure 3. ^{13}C-NMR spectra of PET and its nanocomposite prepared via *in situ* polymerization: (a) Neat PET, (b) PET/FS (2.0 wt%), and (c) PET/MFS(2.0 wt%).

signs such as the chemical shift and the appearance of new peaks in the spectra.

Morphology of PET Nanocomposites. The dispersibility of fumed silica on PET matrix in the nanocomposite was investigated by TEM (Figure 4). The dispersibility of filler is certainly improved as compared with direct melt compounding method[11] regardless of the filler types, and especially, MFS (Figure 4(b)) is more homogeneously dispersed than FS (Figure 4(a)) in the PET matrix. The morphology for the surface of nanocomposite films treated with NaOH solution could be observed by SEM images of Figure 5. These also show that the pore sizes, the traces of silicas removed from film surface, on the surface of PET/MFS film (Figure 5(b)) are smaller and more uniform than those of on the surface of PET/FS film (Figure 5(a)). Thus, these results indicate that the dispersibility of fumed silica on the PET polymer can be improved by the hydrophobic surface modification of filler and in situ polymerization method.
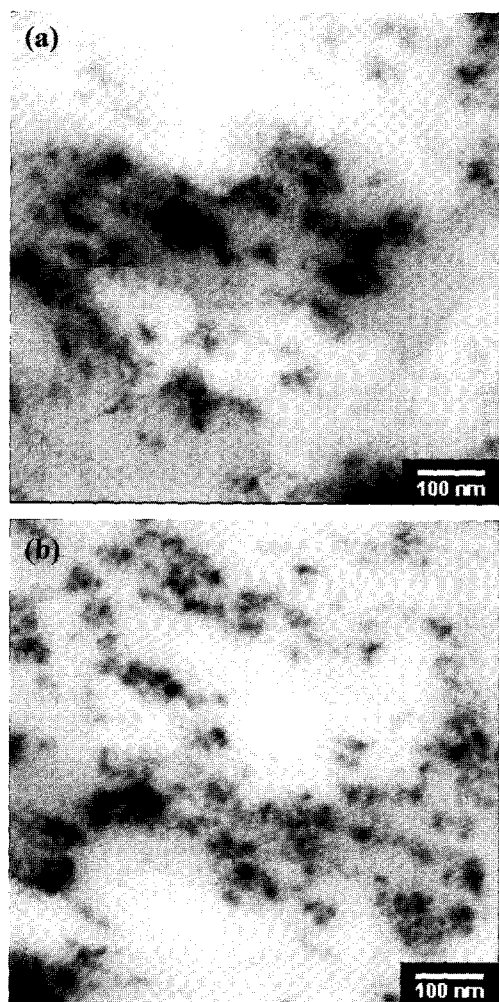
Rheological Properties of PET Nanocomposites. The loss tangent (tan δ) curves for neat PET and its nanocomposites prepared via in situ polymerization at molten state are shown in Figure 6(a). All nanocomposites at the filler content of 2.0 wt% have the lower values of tan δ than those of neat PET, which suggests that the nanocomposites are more elastic than the neat PET over all frequency range at molten state, and the tan δ values of PET/MFS are more decreased than those of PET/FS at a low frequency range.

The Cole-Cole plot in Figure 6(b) also shows that all nanocomposites have lower slopes than 2.0 of neat PET curve at a low loss modulus (G'') value, which indicate that the system of nanocomposites are heterogeneous and much energy would be dissipated.[17] But, over the loss modulus (G'') of about 5×10^3 Pa, the slope of curves for nanocomposites increase and approach to that of neat PET curve. These facts suggest that the system of nanocomposites are changed to isotropic and homogeneous state by shear force, and one of the cause of this result may be the existence of network
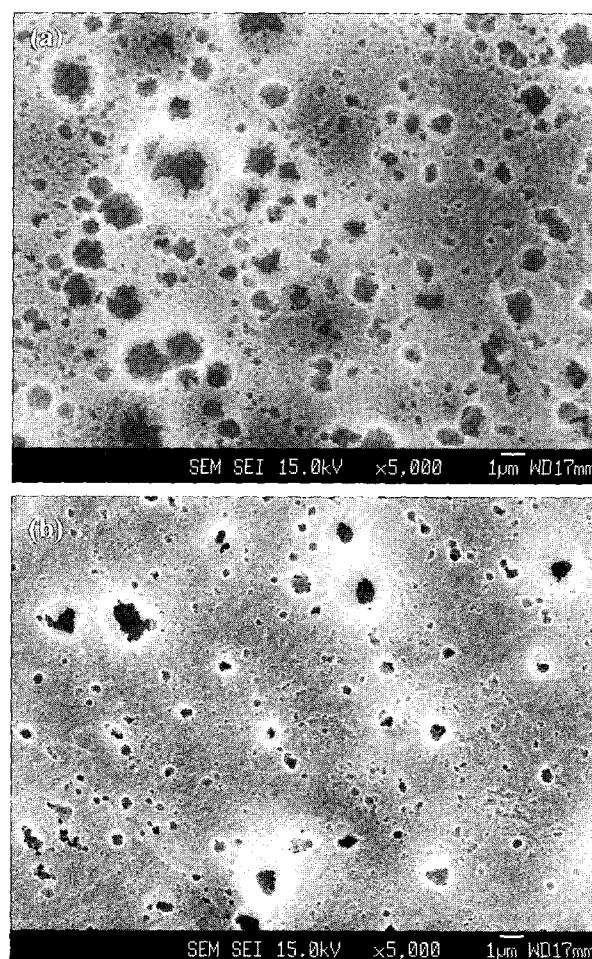

Figure 4. TEM photomicrographs of PET nanocomposites prepared via in situ polymerization: (a) PET/FS (0.5 wt%) and (b) PET/MFS (0.5 wt%).

Figure 5. SEM photomicrographs of NaOH treated surfaces of PET nanocomposites prepared via in situ polymerization: (a) PET/FS (2.0 wt%) and (b) PET/MFS (2.0 wt%).
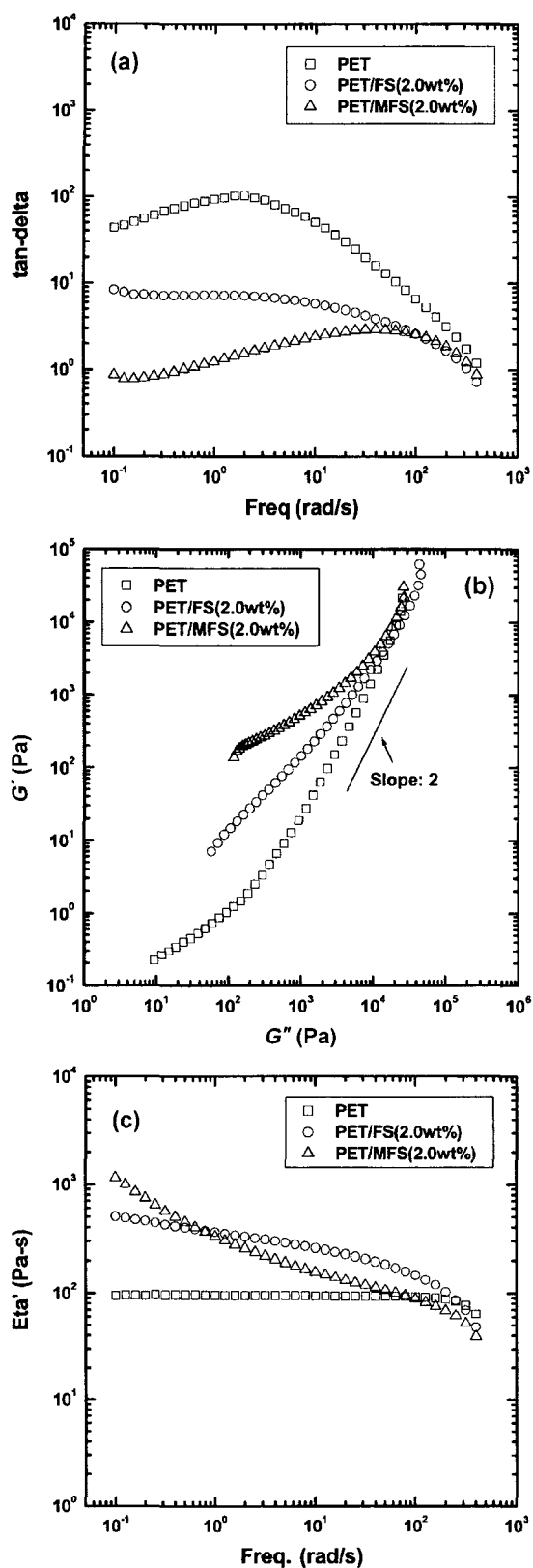
Figure 6. The variations of (a) tan-delta, (b) Cole-Cole plot, and (c) viscosity (Et a) for neat PET and its nanocomposites prepared via *in situ* polymerization (Temperature: 270 °C).

structures due to the particle-particle interaction of fumed silicas in the PET nanocomposites, which can be collapsed by shear force.[7,8,10]

However, these curves of loss tangent (tan δ) and Cole-Cole plot for nanocomposites prepared via *in situ* polymerization change more abnormally than those of nanocomposites prepared via direct melt compounding[11] at the same filler content of 2.0 wt%, and PET/MFS shows the most solidlike elastic properties in this study. These results can be explained by some possibilities: the network structure of filler increases because the dispersibility of all nanoparticles is very effectively improved by *in situ* polymerization, and MFS has more chance to form the structure than FS at the low frequency range and loss modulus (G'') value because MFS has better dispersibility than FS on the PET matrix.

In additon, in the case of viscosity curve as a function of shear force in Figure 6(c), PET/MFS shows also the shear thinning behavior even at a low frequency as expected, but PET/FS dose not conspicuously decrease like PET/MFS as shear force increases and shows the viscosity built up in low frequency. Therefore, these would suggest that FS particles form more agglomeration than MFS on the PET matrix, and this agglomeration can induce the increase of melt viscosity, torque, at the polycondensation for nanocomposites.

Crystallization Behavior of PET Nanocomposites. DSC data in Table III show the characteristic non-isothermal crystallization behaviors of PET nanocomposites against neat PET. The melting peaks (T_m) and the heat of fusion (ΔH_f) of all nanocomposites are almost same as the neat PET regardless of the filler types and filler contents. But, the crystallization temperature (T_c) of all nanocomposites at the second heating shift to high temperature, and the degree of super cooling (ΔT) of all nanocomposites increase except PET nanocomposite filled with FS of 2.0 wt% as compared with neat PET. These behaviors suggest that fumed silicas retard the crystallization rate of PET nanocomposites, and opposite to the results of nanocomposites prepared by direct melt compounding:[11] the fumed silicas acted as nucleating agents in polymer matrix.

In order to investigate this result in detail, isothermal melt-crystallization behaviors were also studied by DSC. The plots in Figure 7 show the variations of the fractional crystallinity, X_t, with time for neat PET and its nanocomposites at various isothermal crystallization temperatures. All fractional crystallinities of nanocomposites are lower than that of neat PET at the same time and the changes of curves are sensitive to temperature. The fractional crystallinity, X_t, at time t can be obtained by Eq. (1).

$$X_t = \frac{\int_0^t (dH/dt)dt}{\int_0^\infty (dH/dt)dt} \tag{1}$$

where the numerator is the area of the exothermic peak at

Table III. DSC Data of Neat PET and Its Nanocomposites Prepared via *in situ* polymerization at Non-isothermal Crystallization

Samples	Filler content [ ]^f (wt%)		$T_c{}^a$ Peak (°C)	$T_c{}^a$ ΔH_c (J/g)	$T_m{}^b$ Peak (°C)	$T_m{}^b$ ΔH_f (J/g)	$T_c{}^c$ Peak (°C)	$T_c{}^c$ ΔH (J/g)	ΔT^d (°C)	$X_c{}^e$ (%)
PET	-		120.3	-27.3	257.9	49.1	197.2	-47.4	60.7	17.3
PET/FS	0.5	[0.51]	130.2	-31.2	258.0	50.5	191.8	-42.8	66.2	15.4
	2	[2.19]	121.5	-33.6	256.6	54.7	201.0	-46.8	55.6	16.8
PET/MFS	0.5	[0.49]	125.4	-31.1	258.9	52.0	186.1	-47.6	72.8	16.6
	2	[2.18]	122.6	-31.0	258.1	53.3	193.2	-46.0	64.9	17.8

^{a}The crystallization temperature measured on the second heating at 10.0 °C/min.
^{b}The melting temperature measured on the second heating at 10.0 °C/min.
^{c}The crystallization temperature measured on the second cooling at 10.0 °C/min. ^{d}The degree of the supercooling: $T_m{}^b$ peak-$T_c{}^c$ peak.
^{e}Apparent crystallinity: $(\Delta H_f - |\Delta H_c|)/\Delta H_f{}^0 \times 100$, $\Delta H_f{}^0$: 125.5 J/g. ^{f}Actual silica content determined by TGA at 750 °C and air atmosphere.

Temperature: 205 ℃
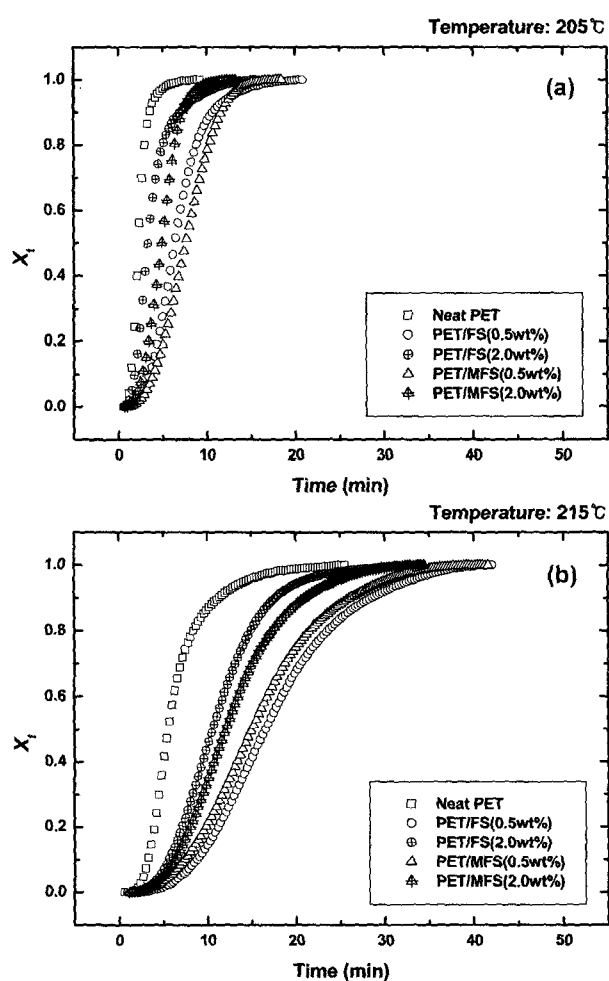

(a)

Temperature: 215 ℃

(b)

Figure 7. The variations of the fractional crystallinity, X_t, for neat PET and its nanocomposites prepared via *in situ* polymerization as a function of time at various isothermal crystallization temperature: (a) 205 °C and (b) 215 °C.

time t and the denominator is the total area of the exothermic peak. The crystallization kinetics of neat PET and its nano-
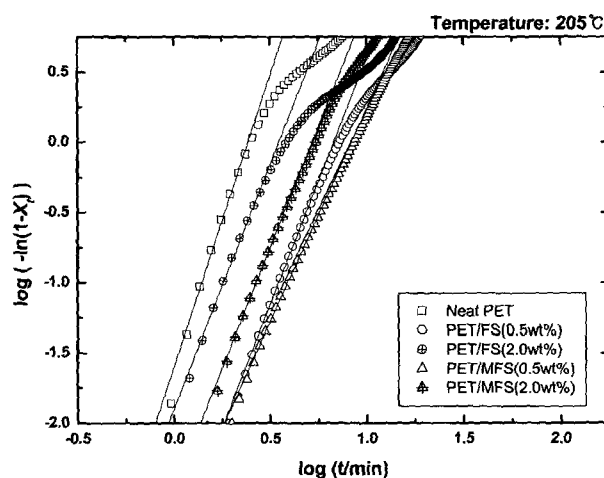
Temperature: 205 ℃

Figure 8. The linear plots of log[-ln(1-X_t)] versus log(t) for neat PET and its nanocomposites prepared via *in situ* polymerization at the primary crystallization (Isothermal crystallization temp.: 205 °C).

composites against time are analyzed in term of the Avrami equation,[18-20] and in this Equation, k is the Avrami rate constant and n is the Avrami exponent, which depend on the nucleation and growth rate of spherulites. The slope of the linear plots of log[-ln(1-X_t)] versus log(t) at the primary crystallization is equal to the Avrami exponent, n, as shown in Figure 8, and the Avrami rate constant, k, is calculated from the half-time of crystallization $(t_{1/2})$.[21]
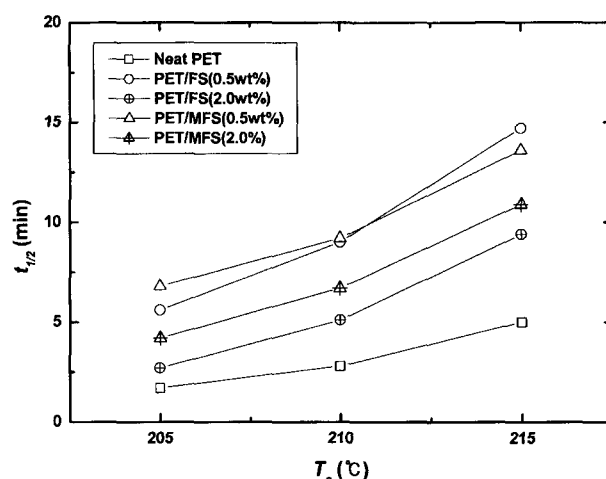
The present study focuses only on primary crystallization and all results are listed in Table IV. These data first show the n values of neat PET are approximately 4 but those of all nanocomposites decrease to nearly 3. According to the Avrami theory, these indicate that the mechanism of crystal growth is changed from homogeneous nucleation to heterogeneous nucleation by the addition of fumed silicas. But, the rate constant k, containing two factors: the nucleation rate and the spherulite growth rate,[22] for nanocomposites notably decrease and their half-time of crystallization $t_{1/2}$ increase.

Table IV. The Avrami Parameters of Neat PET and Its Nanocomposite Prepared via *in situ* Polymerization at Various Isothermal Crystallization Temperature

Samples	Temperature (°C)	$t_{1/2}$ (min)	n	k ($\times 10^{-3}$min^{-n})
Neat PET	205	107	4.0	87.88
	210	2.8	4.0	11.10
	215	5.0	3.9	1.39
PET/FS (0.5 wt%)	205	5.6	3.4	2.03
	210	9.0	3.3	2.03
	215	14.7	3.1	0.18
PET/FS (2.0 wt%)	205	2.7	3.4	23.83
	210.	5.1	3.3	3.56
	215	9.4	3.1	0.71
PET/MFS (0.5 wt%)	205	6.8	3.1	1.81
	210	9.2	2.8	1.33
	215	13.6	2.7	0.63
PETM/FS (2.0 wt%)	205	4.2	3.3	5.97
	210	6.7	3.1	1.82
	215	10.9	3.0	0.50

Figure 9. The variations of the half-time of crystallization ($t_{1/2}$) for neat PET and its nanocomposites prepared via *in situ* polymerization as a function of isothermal crystallization temperature.

These characteristic behaviors mean that the crystallization rate of nanocomposite is definitely lower than that of neat PET, and suggest that fumed silicas retard the crystallization of the PET matrix: the nano-sized fumed silicas hinder the motion of the PET molecular chains to form the crystalline, although the some silicas also act as heterogeneous nucleation sites at first.[13]

Therefore, the reason that these results are opposite to those of nanocomposites prepared by direct melt compounding appears to be related with the improvement of dispersibility of nano fumed silicas via *in situ* polymerization. Because, as shown in Figure 9, almost all the half-time of crystallization, $t_{1/2}$, of PET/MFS are lower than those of PET/FS at the same filler content and same isothermal crystallization temperature, and these values decrease with increasing filler content, which can deteriorate the effective dispersion of

filler and increase the aggregation of filler, regardless of the filler types.

Mechanical Properties of PET Nanocomposites. Mechanical properties of PET nanocomposites as function of filler content and filler type are summarized in Table V. There are no distinct variations in the tensile strength and yield strength of PET and its nanocomposites, and these may be due to the fact that the filler contents of maximum 2.0 wt% are not enough to influence these properties. But, the modulus of all nanocomposites, which is generally related with the wettability and the packing fraction of filler on the matrix,[23-25] increase at low filler content regardless of the filler types, and this reason would indicate the actual maximum packing fractions and packing effect of filler decrease due to the nano-sized fumed silicas.[11,16,26]

Besides, the energy to break point, toughness, of nanocomposites remarkably increases even at the low filler content of 0.5 wt% regardless of the filler types. This result would indicate fumed silicas also interfere the movement of polymer chains during the stress-strain mechanical test, and the processability of PET can be improved by the addition of fumed silica.[27] However, the reason that the modulus and

Table V. Mechanical Properties of Neat PET and Its Nanocomposite Prepared via *in situ* Polymerization

Sample	Tensile Strength (MPa)	Yield Strength (KPa)	Energy to Break Point (mJ)	Young's Modulus (MPa)
Neat PET	63.1 ± 1.5	33.7 ± 3.4	64 ± 18	1316 ± 44
PET/FS (0.5 wt%)	62.7 ± 4.2	30.9 ± 6.6	627 ± 65	1522 ± 68
PET/FS (2.0 wt%)	62.6 ± 3.7	28.1 ± 5.5	247 ± 96	1463 ± 48
PET/MFS (0.5 wt%)	61.4 ± 3.4	29.4 ± 5.3	536 ± 136	1545 ± 67
PET/MFS (2.0 wt%)	63.3 ± 4.6	29.1 ± 4.2	318 ± 83	1493 ± 94

*Mechnical tests were conducted at the cross head speed of 50 mm/min.

the energy to break point of all nanocomposites at the filler content of 2.0 wt% are lower than those at the filler content of 0.5 wt% appear to be caused by the decrease of degree of polymerization, IV, of the nanocomposites.

Conclusions

Thermoplastic PET nanocomposites containing various levels of hydrophilic/ hydrophobic fumed silicas were prepared by *in situ* polymerization. The morphological analysis revealed that *in situ* polymerization is more effective method than direct melt compounding to improve the dispersibility of fumed silicas in the nanocomposites, and hydrophobic fumed silica (MFS) has better dispersibility than hydrophilic fumed silica (FS) on the PET matrix.

BROOKFIELD viscometer and dynamic rheological analysis indicated there are particle-particle interactions of fumed silicas in the PET nanocomposites, and these interactions can increase the melt viscosity of nanocomposites. Various DSC data would suggest that fumed silicas retard the crystallization rate of the PET polymer, and this tendency is related with the improvement of dispersibility for nano filler. Besides, the toughness of PET nanocomposites remarkably increased even at the low filler content regardless of the filler types, which can improve the processability of PET.

References

(1) J. W. Cho and D. R. Paul, *Polymer*, **42**, 1083 (2001).

(2) T. D. Fornes, P. J. Yoon, H. Keskkula, and D. R. Paul, *Polymer*, **42**, 9929 (2001).

(3) Y. Kojima, A. Usaki, M. Kawasumi, A. Okata, T. Kurauchi, and O. Kamigaito, *J. Appl. Polym. Sci.*, **49**, 1259 (1993).

(4) J. H. Chang, B. S. Seo, and D. H. Hwang, *Polymer*, **43**, 2969 (2002).

(5) J. G. Ryu, J. W. Lee, and H. S. Kim, *Macromol. Res.*, **10**, 187 (2002).

(6) P. B. Messesmith and E. P. Giannelis, *J. Polym. Sci., Part A: Polym. Chem.*, **33**, 1047 (1995).

(7) *Technical Bulletin Pigments No. 11*, Degussa-Huls AG, Frankfurt am Main, Germany, 1989.

(8) H. Barthel, *Colloid Surface A*, **101**, 217 (1995).

(9) J. B. Donnet, M. J. Wang, E. Papirer, and A. Vidal, *Kaut. Gummi. Kunstst.*, **39**, 510 (1986).

(10) M. Ettlinger, T. Ladwig, and A. Weise, *Prog. Org. Coat.*, **40**, 31 (2000).

(11) S. C. Chung, W. G. Hahm, S. S. Im, and S. G. Oh, *Macromol. Res.*, **10**, 221 (2002).

(12) E. Reynaud, T. Jouen, C. Gauthier, G. Vigier, and J. Varlet, *Polymer*, **42**, 8759 (2001).

(13) F. Yang, Y. C. Ou, and Z. Z. Yu, *J. Appl. Polym. Sci.*, **69**, 355 (1998).

(14) Z. R. Min, Q. Z. Ming, X. Z. Yong, M. Z. Han, R. Walter, and K. Friendrich, *Polymer*, **42**, 167 (2001).

(15) H. G. Lux, K. Meier, A. Muller, R. Oelmuller, and A. Ramb, US Patent, 6.191.122 B1 (2001).

(16) L. E. Nielsen and R. F. Landel, *Mechanical Properties of Polymers and Composites*, Marcel Dekker, New York, 1994.

(17) C. D. Han, J. Kim, and J. K. Kim, *Macromolecules*, **22**, 383 (1989).

(18) M. Avrami, *J. Chem. Phys.*, **7**, 1103 (1939).

(19) M. Avrami, *J. Chem. Phys.*, **8**, 212 (1939).

(20) M. Avrami, *J. Chem. Phys.*, **9**, 177 (1939).

(21) H. Z. Friendlander and C. R. Frick, *J. Polym. Sci. B*, **2**, 475 (1964).

(22) B. Wunderlich, *Macromolecular Physics: Crystal Melting*, Academic, New York, 1980, vol. 3.

(23) T. B. Lewis and L. E. Nielsen, *J. Appl. Polym. Sci.*, **14**, 1449 (1970).

(24) L. E. Nielsen, *J. Appl. Phys.*, **41**, 4626 (1970).

(25) S. McGee and R. L. McCullough, *Polym. Comp.*, **2**, 149 (1981).

(26) H. S. Katz and J. V. Milewski, *Handbook of Fillers and Reinforcements for Plastics*, Van Nostrand Reinhold, New York, 1978.

(27) J. J. Breuning, R. D. Johnson, and G. K. Morris, US Patent, 531976 (1984).